Journal of Structural Geology 31 (2009) 1238–1254

Contents lists available at ScienceDirect

Journal of Structural Geology

journal homepage: www.elsevier.com/locate/jsg

Multi-scale analysis of Proterozoic shear zones: An integrated structural and geophysical study

John R. Stewart [a,*], Peter G. Betts [a], Alan S. Collins [b], Bruce F. Schaefer [a]

[a] School of Geosciences, Monash University, Building 28, Clayton Campus, VIC 3800, Australia
[b] School of Earth and Environmental Sciences, University of Adelaide, G09, Mawson Laboratories, North Terrace Campus, SA 5005, Australia

ARTICLE INFO

Article history:
Received 13 May 2008
Received in revised form
9 June 2009
Accepted 3 July 2009
Available online 31 July 2009

Keywords:
Aeromagnetics
Forward modeling
Gawler Craton
Gravity
Proterozoic
Shear zone

ABSTRACT

Structural mapping of poorly exposed shear zone outcrops is integrated with the analysis of aeromagnetic and Bouguer gravity data to develop a multi-scale kinematic and relative overprinting chronology for the Palaeoproterozoic Tallacootra Shear Zone, Australia. D_2 mylonitic fabrics at outcrop record Kimban-aged (ca. 1730–1690 Ma) N–S shortening and correlate with SZ_1 movements. Overprinting D_3 sinistral shear zones record the partitioning of near-ideal simple shear and initiated Riedel to regional-scale SZ_2 strike-slip on the Tallacootra Shear Zone (SZ_2). Previously undocumented NE–SW extension led to the emplacement of aplite dykes into the shear zone and can be correlated to the (ca. 1595–1575 Ma) Hiltaba magmatic event. D_4 dextral transpression during the (ca. 1470–1450 Ma) Coorabie Orogeny reactivated the Tallacootra Shear Zone ($SZ_{2\text{-}R4}$) exhuming lower crust of the northwestern Fowler Domain within a positive flower structure. This latest shear zone movement is related to a system of west-dipping shear zones that penetrate the crust and sole into a lithospheric detachment indicating wholesale crustal shortening. These methods demonstrate the value of integrating multi-scale structural analyses for the study of shear zones with limited exposure.

1. Introduction

Lithospheric shear zones record the relative movement histories of crustal blocks (e.g. Elías-Hererra and Ortega-Gutiérrez, 2002). The structural style and sequence of overprinting within these zones provides key kinematic and displacement information which can constrain the relative timing of tectonic transport and deformation, as well as information regarding crustal reactivation and reworking (e.g. Watterson, 1975; Hanmer, 1997; Holdsworth et al., 1997, 2001; Butler et al., 2006). Lithospheric structures form regional patterns in many Archaean–Proterozoic terranes, where their longevity has resulted in complex geological histories (e.g. Culshaw et al., 2006; Williams and Betts, 2009), and increased ambiguity with progressively earlier deformation products becoming obscured or, ultimately, destroyed. The ability to produce accurate and constrained tectonic models and time-integrated reconstructions is therefore reduced in many of these situations. Further, efforts to relate detailed observations within ancient structures to a broader tectonic evolution can be problematic, particularly in data-poor regions such as stable continental interiors dominated by small and isolated basement exposures. The combination of complex overprinting and limited exposure typifies the Gawler Craton of Australia (Fig. 1) where small windows into the deformation history restrict accurate regional interpretations. This is particularly the case within the western Gawler Craton where interpreted curvilinear transpressional zones correlate with regionally continuous, polydeformed shear zones (Teasdale, 1997; Swain et al., 2005a; Fraser and Lyons, 2006; Thomas et al., 2008), within which it is expected that the style and intensity of deformation can vary markedly both across- and along-strike of the regional structures (e.g. Jones and Tanner, 1995; Lin and Jiang, 2001; Czeck and Hudleston, 2003). Consequently, methods that provide some continuity between discrete observations are required.

Regional potential field (aeromagnetic and gravity) datasets have frequently been used for imaging the subsurface (e.g. Bauer et al., 2003) as they can provide a link between outcropping rock and the subsurface (e.g. Whiting, 1986; Betts et al., 2003). The utilization of potential field data to solve 2- and 3-dimensional (2D and 3D) geological problems (e.g. crustal architecture, overprinting relationships and kinematics) has become a powerful tool for tectonic analysis as there is a well-demonstrated relationship between structural geological and geophysical analyses (e.g. Jessell et al., 1993; Jessell and Valenta, 1996; Betts et al., 2003; McLean and

* Corresponding author. Tel.: +61 3 9905 4348; fax: +61 3 9905 4903.
E-mail address: john.stewart@sci.monash.edu.au (J.R. Stewart).

0191-8141/$ – see front matter © 2009 Elsevier Ltd. All rights reserved.
doi:10.1016/j.jsg.2009.07.002

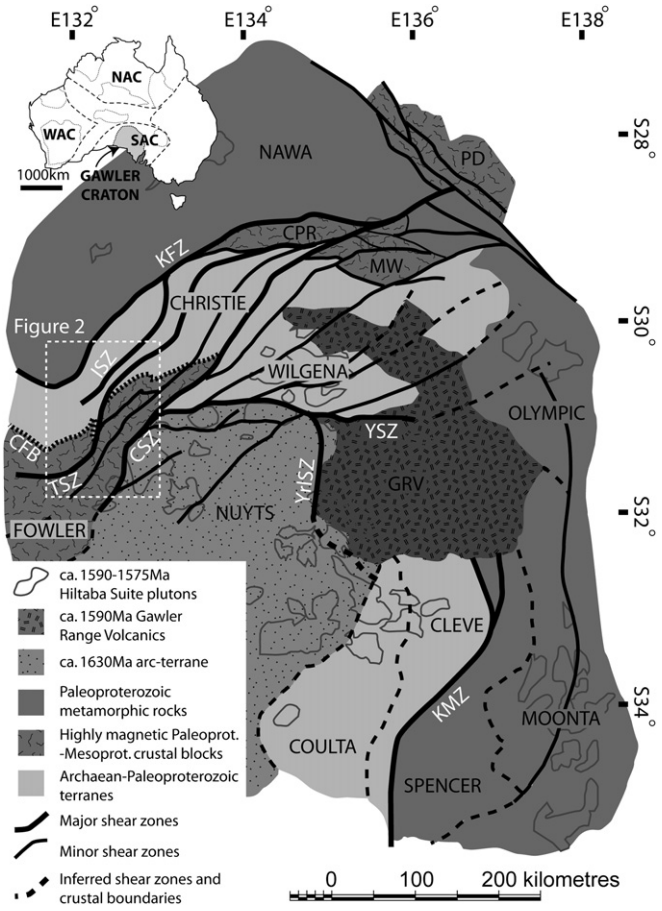

Fig. 1. Interpreted map of Gawler Craton crustal domains (after Ferris et al., 2002; Daly et al., 1998) and distribution of major tectonic elements. Gawler Craton shown with reference to other Proterozoic provinces in Australia (after Myers et al., 1996): WAC – Western Australian Craton; NAC – North Australian Craton; SAC – South Australian Craton. Main structures labeled, from west to east are: KFZ – Karari Fault Zone; ISZ – Ifould Shear Zone; TSZ – Tallacootra Shear Zone; CFZ – Coorabie Fault Zone; YrlSZ – Yarlbrinda Shear Zone; YSZ – Yerda Shear Zone; KMZ – Kalinjala Mylonite Zone. The location of Fig. 9 is indicated by dashed box.

Betts, 2003; Direen et al., 2005a). These types of approaches are invaluable as they: (1) allow a connection between detailed observations at discrete outcrop scales with regional patterns in aeromagnetic data; (2) enable the assessment of the large-scale geological framework to place detailed observations into regional contexts; and (3) can be used to constrain 3D lithospheric architecture at any desired scale.

In this paper we present a structural evolution for poly-deformed rocks exposed within the Tallacootra Shear Zone (Fig. 1). We use the interpreted sequence of events from outcrop to constrain regional structural analysis, produced from the interpretation, modeling and analysis of geophysical data. The Tallacootra Shear Zone is one of the few shear structures in the western Gawler Craton that crops out and allows overprinting relationships to be linked with regional-scale geophysical analysis. Our observations provide a structural framework and relative overprinting chronology as a template for future analyses of the study area. Further, our observations highlight ambiguity in the exclusive analysis of either outcrop or geophysical data in poorly exposed regions. We demonstrate that constraints on tectonic history can be dramatically improved through the integration of outcrop structure with remote and regional interpretations of geophysical datasets.

2. Geological setting of the Tallacootra Shear Zone

Due to extensive Phanerozoic cover within the western Gawler Craton, aeromagnetic and Bouguer gravity datasets have been used to develop terrane and province subdivisions, which define the Nawa, Christie, Fowler and Nuyts Domains (Parker and Hughes, 1990; Parker et al., 1993; Teasdale, 1997) (Figs. 1 and 2). Relevant to this study are the Christie and Fowler Domains, which are separated by a prominent structure herein termed the Christie–Fowler Domain boundary, which is cross-cut by the Tallacootra Shear Zone (Figs. 1 and 2).

2.1. Christie Domain

The Christie Domain is an arcuate province, which is bounded to the north and west by the magnetically prominent Karari Fault Zone and to the south and east by the Christie–Fowler Domain boundary and Coorabie Fault Zones respectively (Fig. 1). Geochronological data suggest that rocks of the Christie Domain were contiguous with the Archaean nucleus (Sleaford Complex) prior to the Proterozoic event framework that affected the Gawler Craton (Swain et al., 2005b; Hand et al., 2007). Archaean Mulgathing Complex rocks make up the bulk of this domain and comprise aluminous metasediments, banded iron formation, quartzite, chert, carbonate and calc-silicate interlayered with metabasic and ultramafic flows and intrusives (Daly et al., 1998). Peak metamorphism reached granulite facies at ca. 2440 Ma during the Sleafordian Orogeny (Teasdale, 1997; Tomkins et al., 2004) which was accompanied by the intrusion of syntectonic granites, tonalites and norites (Fanning, 1997).

The aeromagnetic signature of this terrane is dominated by homogeneously low amplitude responses, disrupted by occasional high intensity circular to elliptical anomalies, interpreted as resulting from the Ifould Suite (Daly et al., 1998; Direen et al., 2005b). Ifould Suite emplacement is accompanied by a syn-shear amphibolite facies mineral assemblage (Teasdale, 1997) and spans the ca. 1730–1690 Ma Kimban Orogeny (Parker and Lemon, 1982; Daly et al., 1998; Vassallo and Wilson, 2001, 2002; Betts et al., 2003; Betts and Giles, 2006; Hand et al., 2007). Narrow highly magnetic bands have been attributed to the presence of banded iron formation (Daly et al., 1998) and form the internal structural grain of the domain. This grain has been reworked into regionally continuous northeast trending shear zones that record ca. 1450 Ma shear ages at Lake Tallacootra and Lake Ifould (Fraser and Lyons, 2006).

2.2. Fowler Domain

The Fowler Domain is unexposed, but has a prominent geophysical response (Fig. 2). It is defined as a northeast trending belt bound by major magnetic and Bouguer gravity gradients, which correspond to the Christie–Fowler Domain boundary to the northwest and the Coorabie Fault Zone to the southeast (Fig. 2d). The internal architecture of this domain is characterized by several discrete crustal blocks with contrasting geophysical signature (Teasdale, 1997; Thomas et al., 2008), which are bound by major magnetic discontinuities interpreted as lower-greenschist to amphibolite grade ductile shear zones (Tomkins et al., 2004) (Fig. 2). This domain has a heterogeneous magnetic response characterized by an overall high amplitude, which is interpreted to be the result of the Palaeoproterozoic intrusion of the Ifould and Tunkillia Suites (Daly et al., 1994; Teasdale, 1997; Ferris et al., 2002,) into high grade and highly magnetic pelitic metasediments (Thomas et al., 2008). The Palaeoproterozoic ages obtained from metasediments within the Fowler Domain are poorly constrained

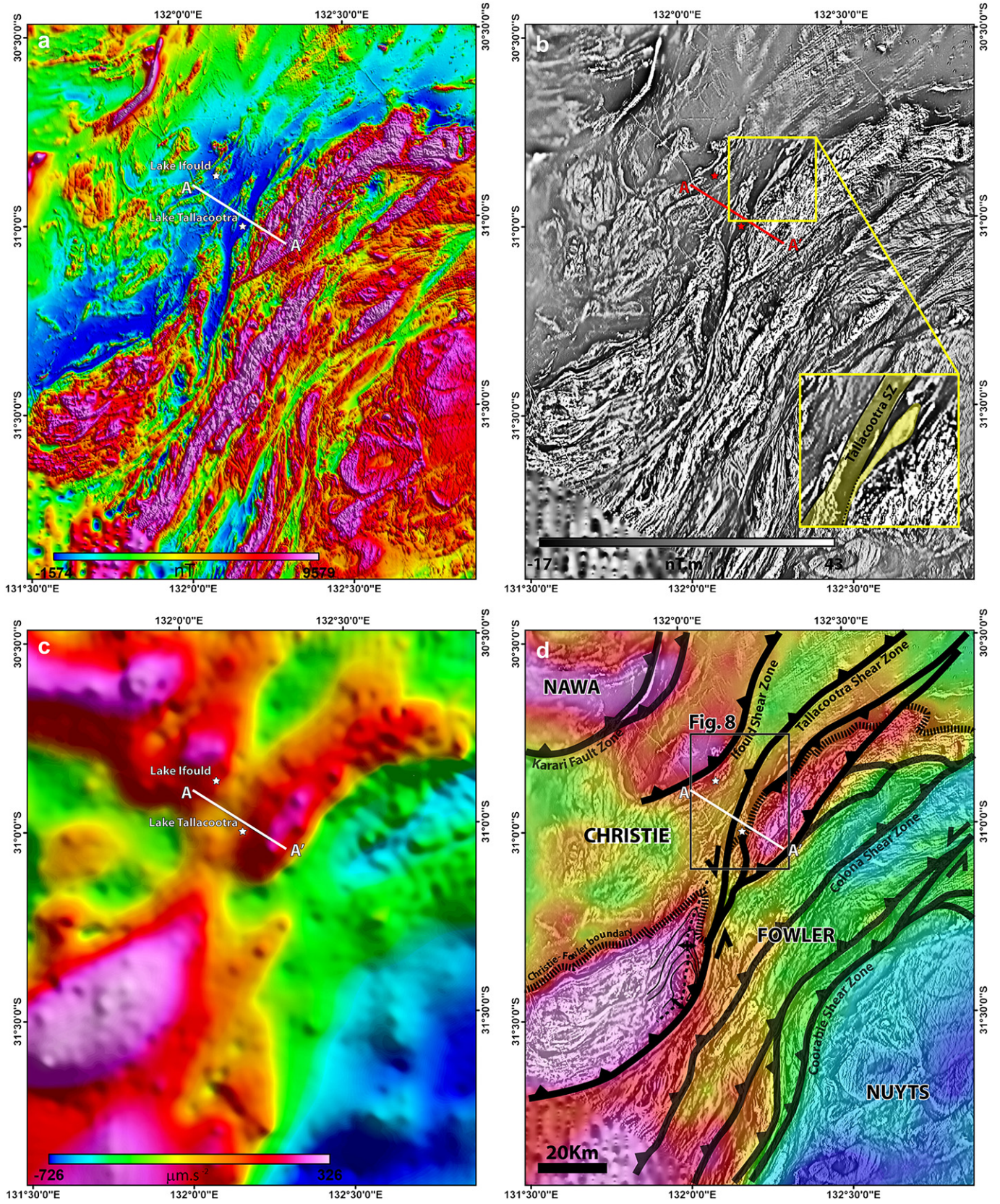

Fig. 2. Processed images of the geophysical datasets for the area shown in Fig. 1. The location of the forward modeled profile (*A*–*A*′) is indicated as well as outcrops at Lake Tallacootra and Lake Ifould. (a) Psuedo-colourdraped RTP image of the aeromagnetic data to highlight the contrasting magnetic intensities and textures between the Christie Domain to the northwest and Fowler Domain to the southeast. (b) Greyscale 1VD of the aeromagnetic data to highlight the structural characteristics of shallow crustal features. Inset and blowup highlights the counterclockwise rotation and attenuation of an interpreted pluton as it approaches the Tallacootra Shear Zone. (c) Psuedo-colourdraped image of the Bouguer gravity data illuminated from the northwest. (d) Composite image of the 1VD data superimposed on the Bouguer gravity to highlight the coincidence of shallow crustal features exhibited by the magnetics with lithospheric gradients exhibited by the Bouguer gravity. Regional interpretation of major shear zone trends and kinematics with fault teeth on the hanging-wall block. Major crustal domains labeled. Box indicates area for detailed interpretation in Fig. 9.

due to a lack of data, which is likely made further ambiguous due to a history of polymetamorphism (Swain et al., 2005a; Thomas et al., 2008). However, a SHRIMP U–Pb zircon date of metagabbro constrains the upper limit for sedimentation to ca. 1726 Ma (Fanning et al., 2007).

Deformed gneisses and BIF near Lake Tallacootra (on the western margin of the Fowler Domain – Fig. 2) have fabrics parallel to the structural grain in aeromagnetic datasets, however, the extent of these sediments and their relationship with mafic and ultramafic rocks is unknown (Daly et al., 1998). The absolute timing of activity along shear zones within the Fowler Domain also remains poorly constrained, with movements constrained to a period between ca. 1680 Ma (Swain et al., 2005a) and ca. 1450 Ma (Fraser and Lyons, 2006). The observed deformation of ca. 1595–1575 Ma Hiltaba Suite granites within the Fowler Domain (Ferris et al., 2002) provides relative movement constraint, confirming some degree of post-1600 Ma crustal reworking. This relative age constraint is supported by widespread ca. 1470–1440 Ma cooling ages (Swain et al., 2005a; Fraser and Lyons, 2006).

2.3. The Tallacootra Shear Zone

The geometry of the Tallacootra Shear Zone has been previously determined based on its interpreted geophysical expression (Teasdale, 1997) and some structural analysis of sparse outcrops at Lake Tallacootra (Teasdale, 1997; Swain et al., 2005a) (Fig. 2). The Tallacootra Shear Zone can be traced from the southern edge of the Australian continental margin northeast to the Coober Pedy Ridge where it intersects the Karari Fault Zone (Fig. 1). While a polyphase evolution has been interpreted for the Tallacootra Shear Zone based on geochronological data (Teasdale, 1997; Swain et al., 2005a; Fraser and Lyons, 2006) the kinematic context is poorly constrained. Apart from the analysis of regional metamorphic field gradients (Thomas et al., 2008), evidence for overprinting relationships and the kinematics of shearing within outcropping rocks has not been adequately demonstrated.

At Lake Tallacootra medium pressure amphibolite facies (600 °C, 6 Kbar: Teasdale, 1997) reworked Archaean mafic granulites and schists of the Mulgathing Complex crop out. Chemical dating of concentrically zoned monazites from Archaean mafic rocks within the Tallacootra Shear Zone yielded bimodal age distributions of ca. 2340 Ma and ca. 1680 Ma (Swain et al., 2005a). The ca. 2340 Ma core ages possibly represent high grade metamorphism during the Sleafordian Orogeny (Swain et al., 2005a). The ca. 1680 Ma rim ages are interpreted as due to deformation along the Tallacootra Shear Zone during the Kimban Orogeny (Swain et al., 2005a) and are contemporaneous with the emplacement of ca. 1670–1680 Ma I-type gneissic to mylonitic granites and pegmatite of the Ifould Suite (Teasdale, 1997; Webb et al., 1986), which have a temporal relationship with the Tunkillia Suite of the central Gawler Craton (Ferris and Schwarz, 2004; Payne, 2008). Aplite dykes cross-cut mylonitic lithologies within the shear zone and represent the latest phase of magmatism recorded at outcrop (Teasdale, 1997). These dykes are folded and weakly foliated, but preserve a well defined mineral lineation, which is in contrast to the strongly foliated and lineated mylonites that they cross-cut Variably mylonitized, foliated to gneissic granites cross-cut Archaean gneisses at outcrops in Lake Tallacootra and ~20 km northwest at Lake Ifould (Teasdale, 1997) (Fig. 2). $^{40}Ar/^{39}Ar$ geochronology yields ca. 1450 Ma ages from shear fabrics at Lake Tallacootra (Fraser and Lyons, 2006). These ages are interpreted to represent a late episode of southeast-directed transport (Direen et al., 2005b) or crustal reorganization and exhumation (Fraser and Lyons, 2006).

3. Geophysical methods

This study utilizes compilations of gridded aeromagnetic and Bouguer gravity data that have been made available in recent years from the South Australian Exploration Initiative and Targeted Exploration Initiative South Australia, Australian Geological Survey Organization, Geoscience Australia and various exploration companies. Aeromagnetic data has been gridded with a 100 m spacing and forms a composite grid of several geophysical surveys with flight line spacing ranging between 250 and 1500 m at acquisition heights between 60 and 150 m above ground level. The aeromagnetic data has had the International Geomagnetic Reference Field (IGRF) removed. Gravity data has an acquisition spacing of ~4000 m and has been gridded with a spacing of 100 m (Fig. 2c).

The gridded datasets were processed and imaged using Oasis Montaj™ software (e.g. Fig. 2). The aeromagnetic dataset has been reduced to the pole (RTP) (Nabighian et al., 2005) (Fig. 2a) and had a first vertical derivative (1VD) filter applied (Nabighian et al., 2005) (Fig. 2b) to enhance high frequency gradients within the data to aid in structural analysis. The Bouguer gravity data has been imaged (Fig. 2c) and layered with the 1VD to demonstrate the coincidence of short wavelength features in the magnetic data with long wavelength features in the gravity data (Fig. 2d).

4. Structural evolution of the Tallacootra Shear Zone

Structural analysis has been undertaken at several localities (e.g. Fig. 3) within mylonitic outcrops at Lake Tallacootra (Fig. 2) to develop a structural and kinematic context with which to constrain the structural analysis of regional aeromagnetic data.

4.1. Early structures

The first generation foliation, S_1, is recognized in relatively low strain zones within reworked Archaean mafic and pelitic gneiss. Although rare, it is preserved within the thickened hinges of F_2 folds and adjacent to D_2 shears (e.g. Fig. 4e) within D_2 drag folds. S_1 is a sub-mm to mm-spaced gneissic foliation defined by the preferred alignment of fine retrogressed biotite-muscovite ± pyroxene and thin quartz-plagioclase ribbons, interpreted as the remnant of partial melting associated with this deformation. D_1 melt is often present as cm-scale rootless isoclinal folds. Thin section analysis of reworked pelitic gneiss indicates that S_1 is preserved as biotite microlithons overprinted by micaceous S_2 cleavage domains (Fig. 5a). F_1 has not been observed within exposures at Lake Tallacootra. The limited number of observations and poor 3D relationships of D_1 structures preclude their detailed structural or kinematic analysis.

4.2. Second generation structures

Second generation structures are characterized by pervasive, tight to isoclinal folding, associated foliation and mylonite development, and boudinage during intense shear zone activity.

S_2 C-foliation is subvertical, gneissic to mylonitic and generally northeast-striking (Fig. 3). Within pelitic gneiss and schist it is defined by pervasive, mm-spaced (0.2–20 mm) segregations of biotite-sillimanite ± garnet and thin ribbons of melt-related quartz ± K-feldspar. Mafic gneiss preserves quartz-plagioclase and biotite-pyroxene fabrics interpreted as S_2. Within these mafic and pelitic lithologies S_2 is interpreted to be S_1-composite due to the intense folding and transposition of first generation surfaces. Mylonitic augen pegmatites and granite preserve thin quartz ribbon structures that enclose plagioclase and K-feldspar porphyroclasts. Fine biotite layers are associated with D_2 shearing and

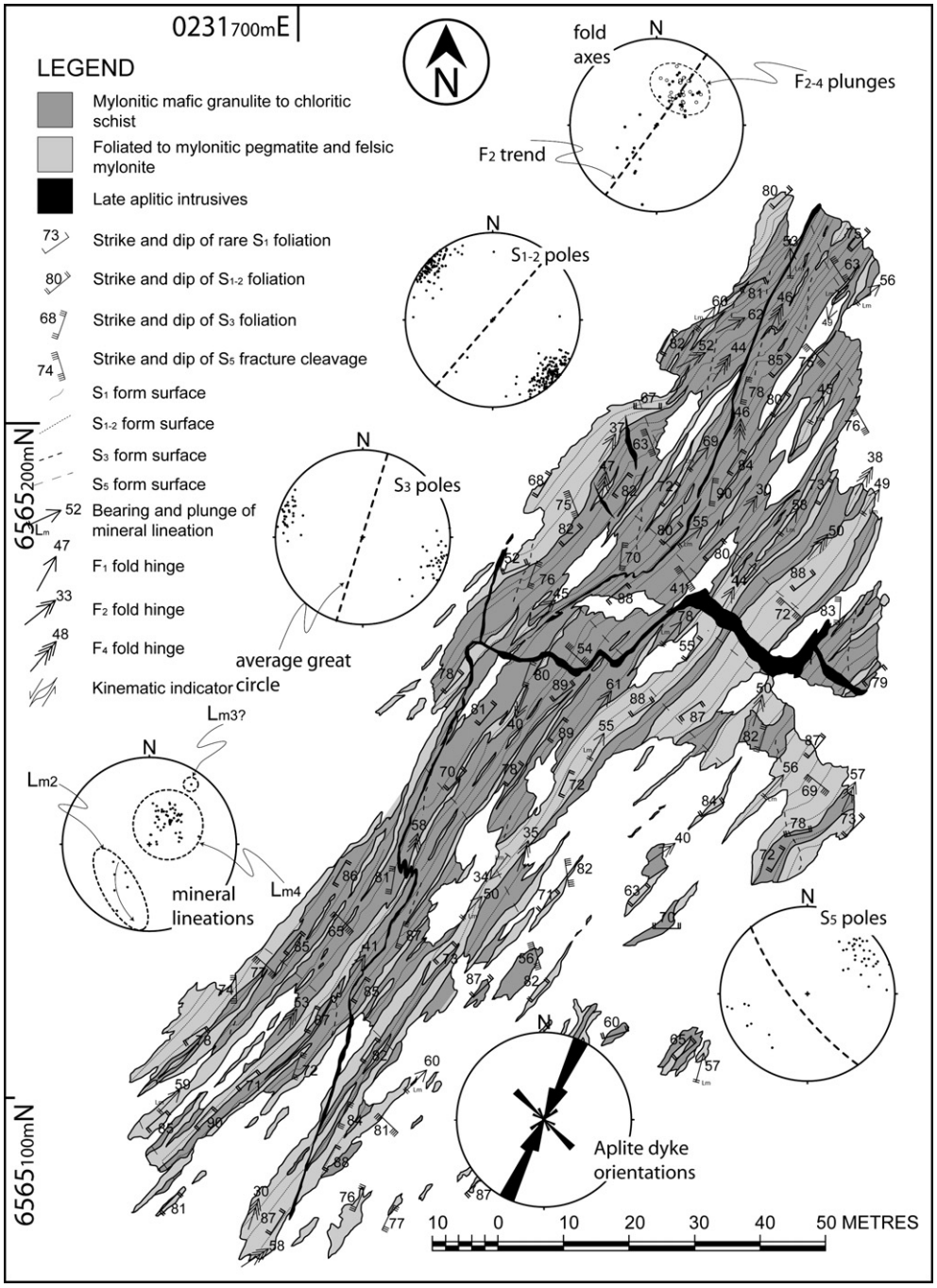

Fig. 3. Map of the main outcropping section of the Tallacootra Shear Zone within Lake Tallacootra. Note strong elongation of felsic lithologies parallel to S_2. Equal area, lower hemisphere stereoplots of major planar (S_{1-4}) and linear (Lm_{2-4}, F_{2-4}) fabric elements. S_5 is a fracture cleavage not referred to in the text.

mylonite development. There is no evidence for D_1 structures within the felsic intrusives so their emplacement is interpreted as pre- or syn-D_2.

Pre- to syn-D_2 partial melts define the limbs of second generation folds (F_2). F_2 folds are isoclinal with cm-scale wavelengths (Figs. 4a,e). Rootless isoclinal folds of partial melts are common within mafic gneiss suggesting strong limb attenuation. The plunges of F_2 fold axes in stereoplots approximate a northeast-striking subvertical great circle that is parallel to the average fabric orientation for S_2 (Fig. 3). Similar trends have been recognized in areas of non-cylindrical folding (e.g. Ghosh and Sengupta, 1984).

Second generation mineral lineations (Lm_2) are characterized by fine mm-spaced aggregates of elongated quartz-feldspar-biotite and are only preserved within mafic gneiss. Lm_2 lineations plunge steeply southwest to shallowly south and are scattered around an S_2-parallel great circle (Fig. 3). This mineral lineation trend has the same distribution as F_2 fold hinges with some poles being deflected to subhorizontal southward plunges. Unlike the F_2 distribution, northeast-plunging Lm_2 are not recognized, possibly due to the overprinting of D_4 mineral lineations.

The limbs of D_2 folded pegmatites have been intensely boudinaged. Associated axial planar cleavages are perturbed within boudin necks and often reoriented into north–northeast strikes by

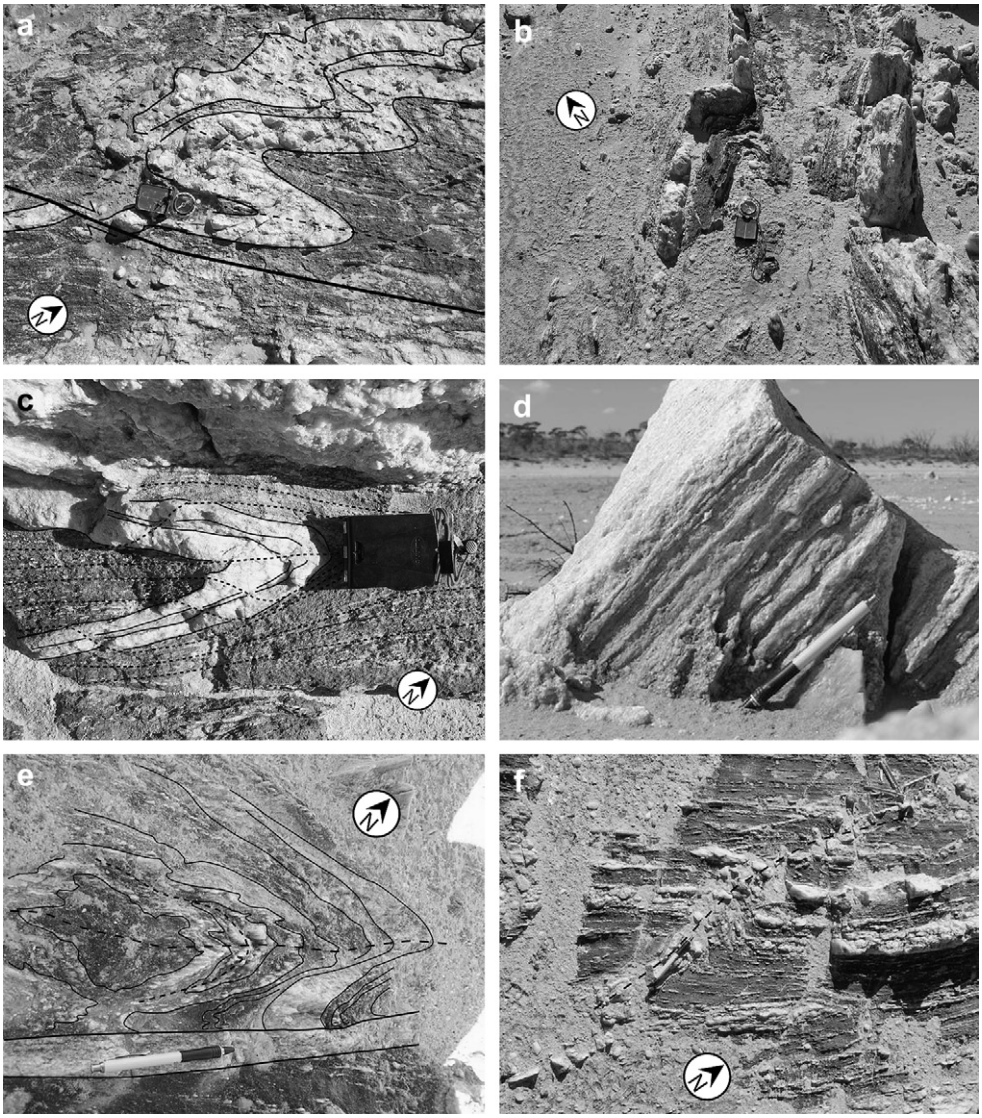

Fig. 4. Structures exposed within pavement outcrops at Lake Tallacootra. (a) Late-D_2 pegmatite within mafic gneiss exhibiting tight F_4 asymmetric folds with dextral vergence. (b) D_4 fold buckling of pegmatitic mylonite in mafic gneiss. (c) Late shear-related D_2 similar fold. Mylonitic fabric parallel to aplite margins is overprinted by cleavage in mafic gneiss. S_4 exhibits fabric distortion as it is refracted through the limbs of the folded aplite. (d) Well defined northeast-plunging Lm_4 mineral lineation consisting of aggregates of elongated quartz and feldspar in pegmatitic mylonite. (e) Flow perturbation refolding in footwall of a cm-scale northeast trending late-D_2 mylonite preserving a strong component of flattening. (f) F_4 asymmetric folds of D_2 leucocratic veins in mafic gneiss. Sigmoidal axial plane is parallel to S_3.

localised sinistral shearing. These structures occasionally develop into sinistral shears that are interpreted to have formed during D_3. Within pavement outcrops of mafic gneiss, asymmetric and boudinaged fabric parallel leucosomes exhibit both apparent dextral and sinistral asymmetries suggesting either overprinting shearing events or a strong component of dip–slip movement. Kinematics are thus difficult to establish within mafic gneiss at outcrop as the horizontal viewing plane is likely mis-oriented relative to D_2 kinematic indicators. Asymmetric porphyroclasts preserved in granitic and pegmatitic blocks record σ-type and δ-type clasts and indicate both west-side and east-side-up shear sense.

Rare, cm-scale ductile shear zones trend NE–SW (Fig. 4e) and contain C' fabrics exhibiting west-up (Fig. 5b) and east-up shear senses possibly due to strong flattening D_3 shear zones are defined by a D_2 mineral assemblage, are mylonitic and contain thin relict melt veins. Where recognized, these shears truncate D_1 and syn-D_2 pegmatite and locally perturb S_2 fabrics indicating that they began propagating after S_2 had been established.

At Lake Tallacootra structures that formed during D_2 deformation indicate northwest–southeast oriented shortening, the kinematics of which are ambiguous. D_2 has a lower age limit constrained by the emplacement of ca. 1680 Ma granites and pegmatites that were deformed within the shear zone. An upper age limit is constrained by aplite dykes that cross-cut the mylonitic D_2 foliation, however dating of these intrusives remains inconclusive (Fanning et al., 2007).

4.3. Third generation structures

Structures developed during the third deformation (D_3) are subtle at outcrop scale and exhibit cm- to m-scale spacing. Third generation fabric elements (S_3) are defined by mm-scale north–northeast trending, subvertical quartz-K-feldspar leucosomes, quartz veins and occasional cm-scale mylonite bands (Fig. 5e). In thin section, partitioned zones of sinistral micro-shearing are associated with thin biotite-dominated zones within pelitic gneiss

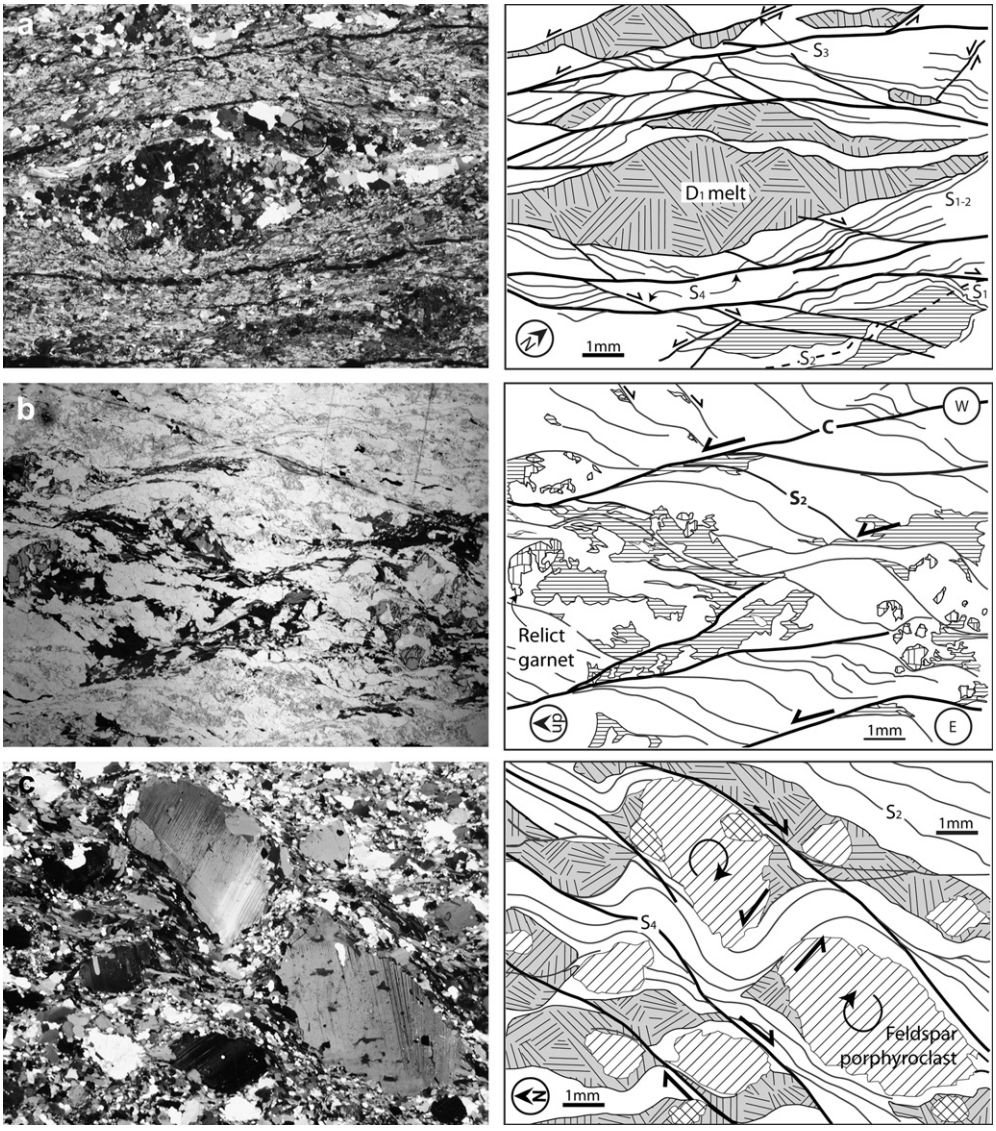

Fig. 5. Photomicrographs of thin sections (left) with sketches showing main fabric elements (right). (a) Retrograde overprinting of D_2 fabrics and D_3 sinistral shears by anastamosing D_4 microshears within chloritic quartz-feldspar-biotite-muscovite ± garnet schist. Note F_2 fold hinge in eastern corner. Crossed polars. (b) Quartz-kspar-biotite ± garnet mylonite with a well developed S–C fabric. S_2 fabric and quartz melts are dragged into D_3 west-side-up C planes. Plane polarized light. (c) Quartz-feldspar-biotite-garnet protomylonite with recrystallised quartz matrix and D_2 muscovite-biotite fabric wrapping around twinned K-feldspar porphyroclasts. Clockwise rotation of porphyroclasts is accompanied by antithetic sinistral shear during dextral movement on S_4 surfaces. Crossed polars.

(Fig. 5a). Centimeter-scale aplite dykes cross-cut S_2 and are often aligned with S_3 (Fig. 3). Folding associated with D_3 is not observed at the outcrop scale.

D_2 boudin necks are commonly separated by cm-scale discrete sinistral ductile shears (Figs. 6 and 7), which locally perturb S_2 foliation and are interpreted as the cause for the spread of S_2 poles (Fig. 7). This shearing is interpreted to occur during D_3 and is related to distributed cm- to m-scale displacements.

A shallowly northeast-plunging mineral lineation is attributed to sinistral movements during this episode implying strike-slip movement, although large strike-slip displacements are not observed in outcrop. The strike-slip movement along D_3 shear zones provides a mechanism for local flow perturbation and re-orientation of F_2 and Lm_2 from moderate to shallow plunges (Fig. 3). Within thin section there is evidence for a component of partitioned west-side-up movements (Fig. 5b).

The emplacement of S_3-parallel quartz veins and aplite dykes suggests that north–northeast trending S_3 surfaces accommodated oblique extension orthogonal to the bulk northwest–southeast trending shortening direction within the shear zone (Fig. 6). The characteristics and geometries of all structures attributed to D_3 suggest a component of northeast–southwest oriented extension.

4.4. Reactivation

An episode of renewed deformation is well-preserved in felsic intrusives within Tallacootra Shear Zone outcrops, the characteristics of which are best observed in post-D_2 aplite dykes.

S_3 fabrics and prominent S_3-parallel aplite dykes are truncated by S_4 surfaces, which are parallel to and rework S_2 and D_2 mylonite (e.g. Fig. 8). S_4 cleavages are spaced within mafic gneiss and schist preserving a retrograde (quartz-muscovite-chlorite-epidote) mineral assemblage (Fig. 5c). In thin section S_4 dissolution cleavages appear to be contemporaneous with muscovite growth (e.g. Fig. 5a). Thin sections of pelitic gneiss and schist reveal muscovite overgrowing

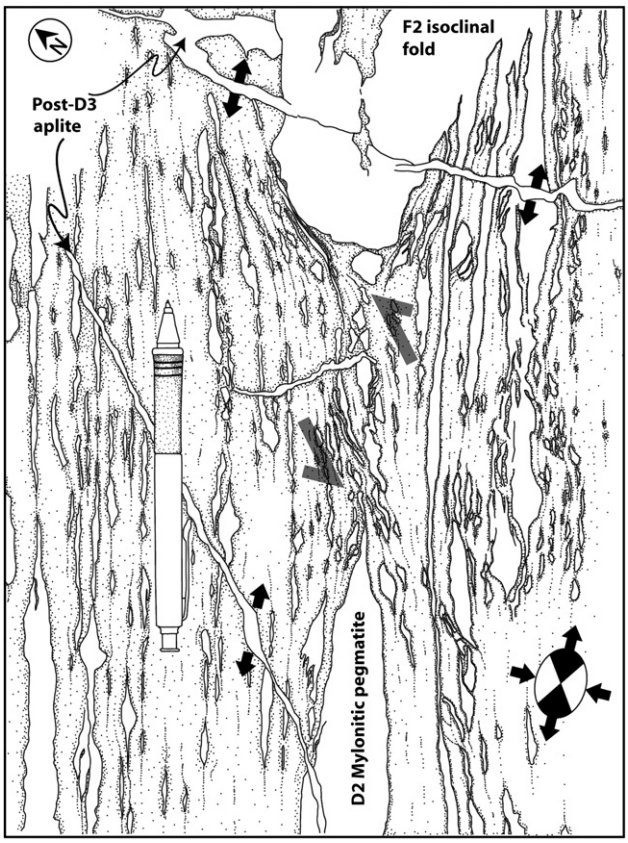

Fig. 6. Sketch of pavement outcrop within the Tallacootra Shear Zone. Boudin of D_2 granitic mylonite is a sinistrally offset limb of the isoclinal fold to the northeast. Thin aplitic veins are parallel to D_3 sinistral shear zone and indicate a component of extension subparallel to the main S_2 fabric within the shear zone as shown by the schematic ellipse.

biotite within D_2 shear planes accompanied by new muscovite growth in C planes.

Shear-related folds or buckles are the most easily distinguishable structures from pre-existing generations. F_4 asymmetric buckle folds (e.g. Fig. 4b) generally affect bands of felsic mylonite with high aspect ratios and strike lengths of several meters (e.g. Fig. 8). They also occur through fabric instabilities associated with the reactivation and slip on S_3 surfaces (e.g. Fig. 4f) and are interpreted to form under partitioned simple shear similar to that described by Mandal et al. (2004). Their sigmoidal axial traces indicate that they are consistently synthetic to a component of dextral shear (e.g. Carreras et al., 2005). Late-D_2 mylonite and S_3-parallel aplite dykes occasionally form tight, similar F_4 folds (Figs. 2a,c), the axial planar dissolution cleavage of which is often refracted through the fold limbs (Fig. 2c). All F_4 fold axes plunge moderately northeast (Figs. 3 and 8).

A prominent mineral lineation (Lm_4) is preserved within mylonitic pegmatite (Fig. 4d), within leucocratic-rich domains in mafic and pelitic gneisses, and within post-D_3 L-tectonitic aplite dykes. Lm_4 primarily comprises mm- to cm-scale elongated aggregates of quartz-feldspar-biotite. These lineations have consistent plunges to the northeast parallel to D_4 fold axes (Figs. 3 and 8).

In outcrop, kinematic evidence for D_4 is restricted to reactivated S_2 fabrics and some mylonitic pegmatite associated with renewed shearing. North–northeast trending aplite dykes within the southwest outcropping area are slightly sigmoidal in shape indicating localised dextral shear (Fig. 8). Asymmetric porphyroclasts and discrete *C′* fabrics within pegmatitic mylonite indicate east-side-up kinematics and are clearly stretched parallel to Lm_4. Dextral kinematics observed on pavement outcrops are related to the component of dextral movement associated with oblique east-up movements.

D_4 kinematics indicate northwest–southeast oriented shortening within the shear zone outcrops coupled with a component of oblique dextral shear. The bulk movements suggest that a shallowly southeast plunging axis of clockwise vorticity aided east-side-up movements of the western Fowler Domain with respect to the Christie Domain.

5. Geophysical Interpretation

Of the numerous regional-scale discontinuities within the Christie and Fowler Domains the Tallacootra Shear Zone is the most favorable to test the ability to correlate the scale of structural relationships as it is one of the few shear zones that outcrop. Our geophysical analysis and interpretation is focused primarily on this structure and the crustal blocks adjacent to it.

Structural interpretations are made based on the following assumptions: (1) aeromagnetic anomalies are the product of lithological contrasts within the shallow crust, therefore; (2) linear aeromagnetic fabrics are the products of deformation on horizontal axes (e.g. shortening, tilting, folding or faulting of a stratigraphic package with internal magnetic contrasts); (3) truncations or deflections of magnetic anomalies indicate the location of a fault or shear zone; (4) rotation or offset of marker anomalies indicates the apparent strike-slip separation; and (5) gradients within the potential field datasets can serve as a proxy for the dip direction of sources to magnetic and gravity anomalies whereby, with respect to a single linear anomaly, the side with the shallower gradient indicates the direction of dip.

5.1. Geophysical characteristics of the Tallacootra Shear Zone

The Tallacootra Shear Zone forms a regionally persistent, curvilinear anomaly as imaged in the aeromagnetic data, and occurs along magnetic strike of outcropping mylonitic rocks at Lake Tallacootra (Fig. 2). It has a typically high frequency aeromagnetic response that exhibits along-strike variations (Fig. 2a). This high frequency expression is superimposed on low amplitude magnetic responses within the Christie Domain and highly amplitude responses within the Fowler Domain forming a zone ranging in width from 500 to 3000 m. The anomaly is curved, but generally northeasterly trending within the Christie and Fowler Domains, A north–northeasterly trending segment incorporates the zone of outcrop at Lake Tallacootra and forms a ~35 km long boundary between the Christie and Fowler Domains (Fig. 2d). Calculations of the vertical gradients within the aeromagnetic dataset highlight the attenuation of magnetic anomalies exhibited within the Fowler Domain (Fig. 2b). Within the Christie Domain moderately to highly magnetic, oblate to strongly elliptical bodies increase the typically low aeromagnetic response of the domain. One such anomaly can be seen to bend into the shear zone becoming increasingly attenuated toward the south–southwest providing apparent sinistral kinematics along the north–northeast trending segment (Fig. 2b – inset). These kinematics are confirmed by ~40 km of apparent offset of the folded Christie–Fowler Domain boundary (Fig. 2d). The asymmetry of regional aeromagnetic gradients across the interpreted shear zone indicate that this structure changes dip alongstrike. Northeasterly trending segments within both the Christie and Fowler Domains dip steeply to the northwest, whereas the north–northeasterly trending segment is subvertical to slightly east–southeast dipping (Fig. 2d).

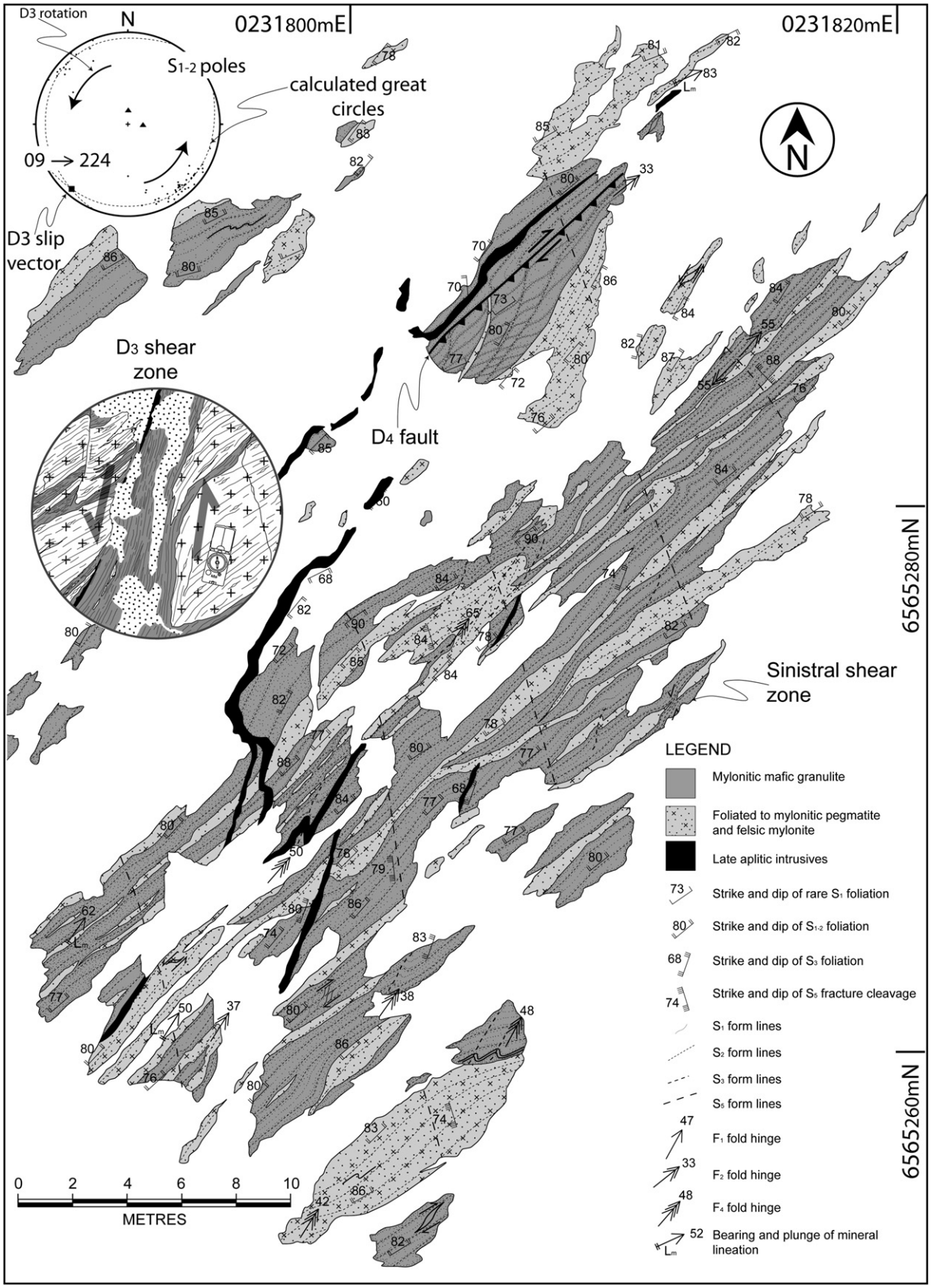

Fig. 7. Detailed map of the northern part of the main outcropping section of the Tallacootra Shear Zone within Lake Tallacootra. Lower hemisphere, equal area stereoplot with local distribution of S_{1-2} indicating counterclockwise rotation and strike-slip during D_3. Inset blowup of D_3 sinistral shear zone truncating D_2 pegmatitic mylonite.

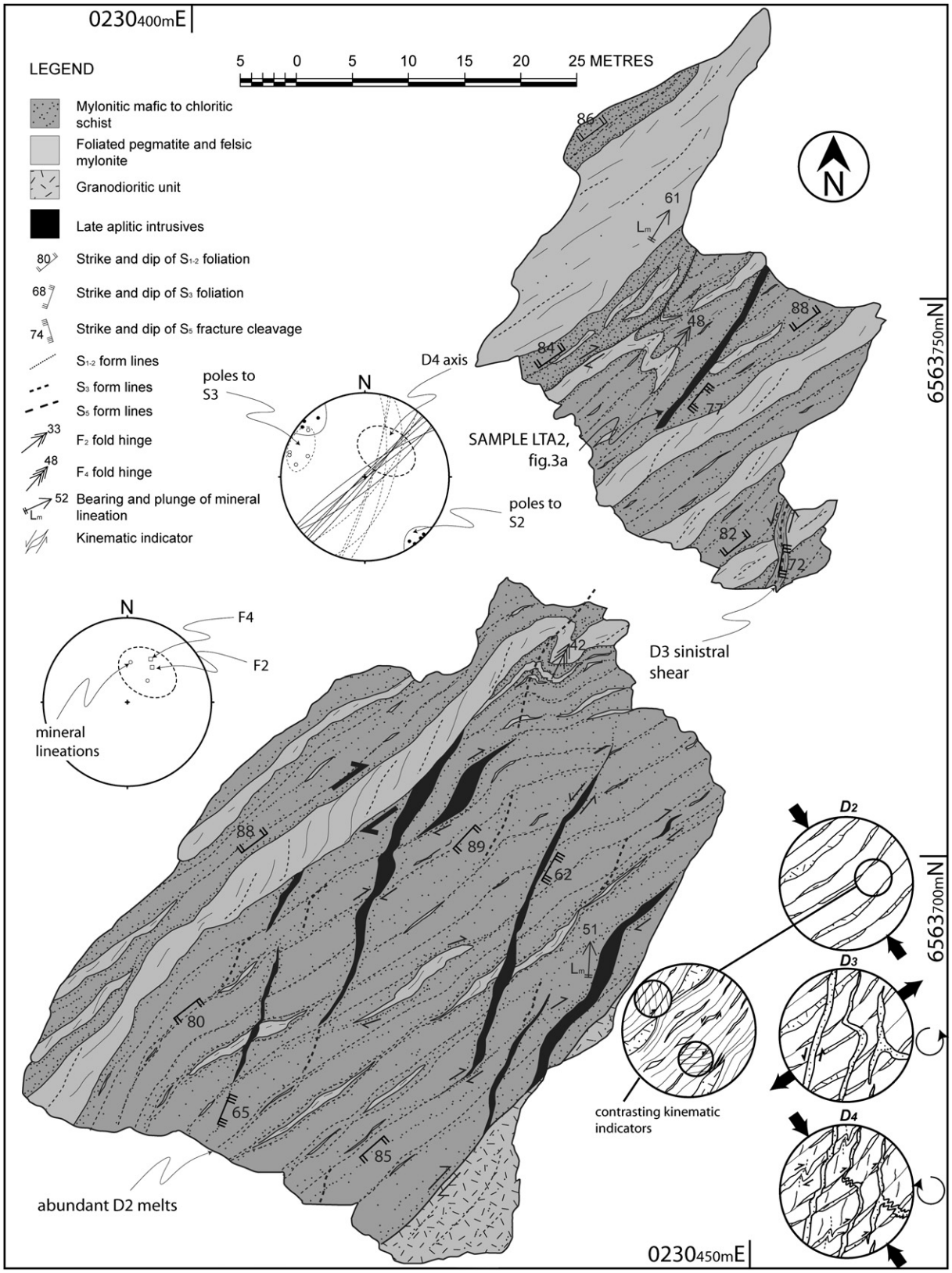

Stewart et al. Figure 8

Fig. 8. Detailed sketch-map of a discrete outcrop located on the southwestern edge of Lake Tallacootra. Equal area, lower hemisphere stereoplots highlight the NE-plunging D_4 axis. Insets show schematic evolution of D_2–D_4 shear zone fabrics with interpreted shortening and vorticity components.

The interpreted location of the Tallacootra Shear Zone as defined using aeromagnetic data is confirmed within images of the Bouguer gravity data (Fig. 2c). The shear zone clearly coincides with regional gradients within the Bouguer gravity highlighting the juxtaposition of crustal blocks with contrasting densities. The largest gravity gradient occurs in the vicinity of Lake Tallacootra where high gravity values of the western Fowler Domain (50–90 μm s^{-2}) contrast with low gravity values of the Christie Domain (−30 to −80 μm s^{-2}). The positive gravity anomalies associated with the western Fowler Domain are sinistrally offset along the north–northeasterly trending segment of the Tallacootra Shear Zone (Fig. 2d) confirming the kinematics observed within the aeromagnetic data.

Approximately 15–20 km northwest of the outcrops at Lake Tallacootra a distinctive northeast trending curved zone of low magnetic amplitude occurs (Fig. 9a). This anomaly is between 3 and 5 km in width and coincides with a regional Bouguer gravity gradient that separates a dense crustal block to the northwest from lower density crust to the southeast (Fig. 2d). This anomaly has previously been interpreted as a splay of the Tallacootra Shear Zone (Teasdale, 1997), however there is no evidence for connectivity within the aeromagnetic or gravity data (Fig. 2d). This structure is herein referred to as the Ifould Shear Zone.

5.2. Overprinting and structural architecture

The interpretation of aeromagnetic data over a detailed area (Fig. 9a) has allowed the discrimination of structural overprinting phases. The complex, often anastamosing relationships of interpreted faults within Fig. 9b can be related to a combination of shear zone overprinting and reactivation, which is simplified in Fig. 9e.

The earliest generation structures (SZ_1) are interpreted as parallel to the Christie–Fowler Domain boundary (Fig. 2d). These structures only exhibit prominence within the Fowler Domain where they separate crustal blocks of varying magnetic intensity (Fig. 9a). They also show a close relationship to the location, and are parallel to the elongation, of interpreted Ifould Suite plutons. Within the interpretation area, SZ_1 faults are curved and appear reworked by later generation structures, although the geometry of reworking is difficult to quantify in 2D. Within the Christie–Fowler Domain boundary zone (~5 km wide), several of these faults are interpreted to dip steeply toward the southeast. The movement on SZ_1 may be temporally related to the emplacement of Ifould Suite plutons, which are deformed by and partially overprint these structures.

SZ_2 structures trend northeast to north–south and include the Tallacootra Shear Zone (Fig. 9b). Establishing the relative position of second generation shear zone (SZ_2) movements within a deformation framework for the interpretation area (Fig. 9a) has only been applicable to the Tallacootra Shear Zone as SZ_2 shear zone movements appear highly partitioned and only occur within discrete zones at the scale of Fig. 9b. Although the trend of the Ifould Shear Zone (Fig. 9b) shares many similarities with the Tallacootra Shear Zone at the regional-scale (see Fig. 1), the same sequence of overprinting is not observed for this structure. However, SZ_1 structures

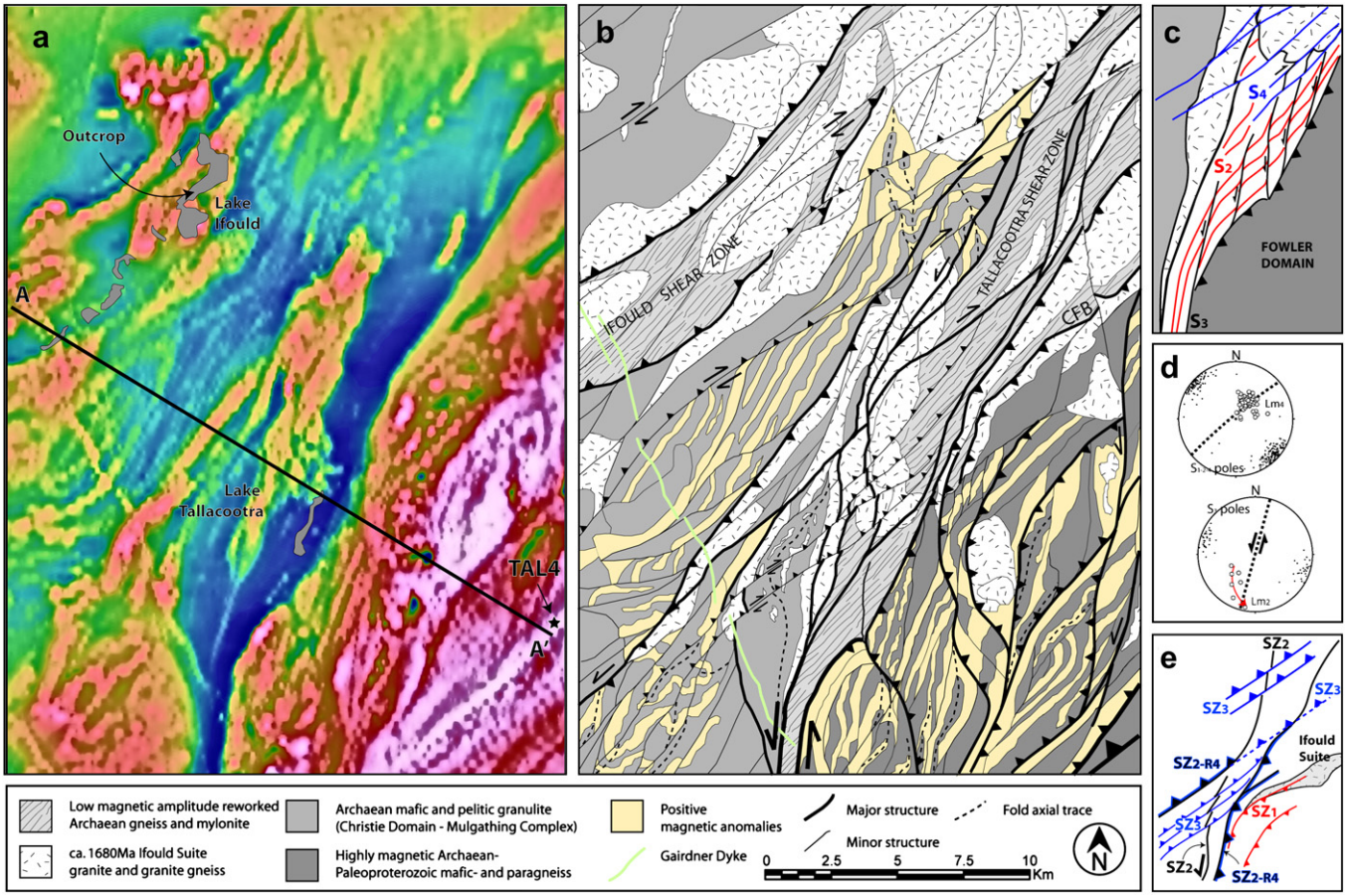

Fig. 9. Detailed aeromagnetic interpretation of the Lake Ifould and Lake Tallacootra area. Location shown in Fig. 2d. (a) 1VD of the aeromagnetic data superimposed on the RTP. Locations of outcrops at Lake Tallacootra and Lake Ifould shown in grey. The location of profile *A–A′* is placed with the position of drillhole TAL4. (b) Structural interpretation for the area in (a). Fault teeth on hanging-wall blocks. (c) Schematic summary of the main fabrics recognized at outcrop. (d) Summary equal area, lower hemisphere stereoplots of the main fabrics within shear zone outcrops. (e) Schematic interpretation of the overprinting shear zone generations within the structural interpretation. Correlation with the fabric generations at outcrop is shown in Table 3.

and interpreted plutons within the Christie–Fowler Domain boundary zone curve towards the Tallacootra Shear Zone exhibiting a sinistral sense of apparent movement along north–northeast to north–south trending segments. The SZ_1 structures within the Fowler Domain are ultimately truncated by the Tallacootra Shear Zone, which becomes the boundary fault between the Christie and Fowler Domains at the southern extent of Fig. 9b. It is important to note here that the dominant shear zone fabrics at outcrop within Lake Tallacootra trend northeasterly (oblique to the eastern boundary of the Tallacootra Shear Zone) and are overprinted by partitioned zones of sinistral shearing that trend north–northeasterly to north–south (Figs. 9c,d). This suggests that the main fabric within the shear zone outcrops (S_2) records a shearing event that predates the inception of movement on this north–northeast trending segment of the Tallacootra Shear Zone.

Sets of slightly curved, northeast trending, northwest-dipping faults (SZ_3) cross-cut SZ_2 structures in the vicinity of Lake Tallacootra (Fig. 9b). These faults often splay off northeast trending segments of curved, SZ_2 structures (e.g. southern boundary fault to the Ifould Shear Zone) and overprint fault segments with northerly strikes. Apparent dextral and sinistral strike-slip offsets on SZ_3 structures conflict with predominantly dextral drag senses indicating a significant component of dip–slip. SZ_3 faults that overprint the Tallacootra Shear Zone are themselves truncated by the eastern margin of this structure. This overprinting relationship suggests that a separate movement phase can be attributed to the reactivation of north–northeast trending, east dipping structures such as the Tallacootra Shear Zone or they may represent an earlier fault phase. This interpreted reactivation (SZ_{2-R4}) appears to be focused at the margin of the Christie and Fowler Domains affecting the north–south to north–northeast trending segment of the Tallacootra Shear Zone, and optimally oriented SZ_1 structures within the Fowler Domain (Fig. 9b).

6. Forward modeling

Reduced-to-pole aeromagnetic and Bouguer gravity data have been extracted along a ~32 km section perpendicular to the interpreted strike of the Tallacootra Shear Zone (Figs. 2a,c). These data have been forward modeled along a 2D profile that extends to 50 km depth using GmSys™ modeling software. This modeled depth extent has been selected to address the long wavelength gradients within the aeromagnetic and Bouguer gravity data between the Christie and Fowler Domains (i.e. across the Tallacootra Shear Zone – Fig. 2c). Interpreted surface structural and lithological trends are extended into the profile based on the mapped patterns in Fig. 9b. Published average densities for major lithologies within the WGC (Direen et al., 2005b; Thomas et al., 2008) have been used to constrain our forward model (Table 1). All measured densities are from exposed basement and shallow drillholes and thus provide minimum values for modeling on a lithospheric scale based on the assumption that a natural increase in density occurs with increasing depth. Magnetic susceptibility data for the Christie and Fowler Domains has been compiled from various sources (e.g. Teasdale, 1997; Thomas et al., 2008; and this study) and is presented in Table 2.

6.1. Profile A–A′

A regional (~20 km wavelength) positive Bouguer gravity anomaly (peak = 9.9 μm s^{-2}) coincides with eastward-increasing regional magnetic values within the Fowler Domain (Fig. 10). In contrast, the Christie Domain, to the west, is characterized by a regional gravity trough (−6 to −7 μm s^{-2}) and a relatively negative magnetic response (~200 nT) (Fig. 10). The primary gradients within both the gravity and magnetic data indicate significant lithospheric scale contrasts between the rock properties of these two domains. Within the Christie Domain, between 35 and 40 km of total crustal thickness is modeled to account for the low Bouguer gravity values. Within the Fowler Domain, high density mantle lithosphere is modeled to underlie a reduced crustal thickness of between 5 and 15 km where Palaeoproterozoic mafic and pelitic granulites reside in the near surface (Thomas et al., 2008). Superimposed on the regional magnetic anomalies are positive, short wavelength disparities. Within the Christie Domain these local anomalies correspond to interpreted dolerite dykes and sheared fault-bounded Ifould Suite granites (Fig. 9b). Within the Fowler Domain short wavelength, negative anomalies coincide with interpreted shear zones (SZ_1), the dip directions of which are constrained by the magnetic data. The interpreted shear zones bound crustal slices, which are characterized by contrasting magnetic amplitudes (Fig. 10). These contrasts have been modeled as the result of differential exhumation of a Palaeoproterozoic supracrustal package, which incorporates a dense (2770–3010 kg m^{-3}), magnetic (0.013–0.111 SI), interpreted granulite grade mafic and pelitic layer, underlying a less dense (2750–2880 kg m^{-3}), less magnetic (0.009–0.046 SI) metasedimentary layer.

The lithospheric architecture within the western Fowler Domain resembles a positive flower structure (e.g. Woodcock and Rickards, 2003) bound in the west by an east dipping segment of the Tallacootra Shear Zone that forms the boundary between the Christie and Fowler Domains. At ~30 km depth, the Tallacootra Shear Zone is interpreted to splay from a major west-dipping structure, which forms the eastern boundary of the flower structure and soles into a detachment at the base of the crust at ~43 km. Within the Christie Domain sets of west-dipping SZ_3 faults truncate magnetic sources and interpreted granites within the upper 10–15 km. In the eastern section of the modeled Christie Domain these faults are overprinted by major east-side-up steeply dipping shear zones (SZ_{2-R4}) that are kinematically related to the latest movement on the Tallacootra Shear Zone. In the western section of the Christie Domain SZ_3 faults have been modeled as reactivated splays (SZ_{3-R4}) from the lithospheric structures with an activity interpreted as contemporaneous with west-side-up movements on the Ifould Shear Zone.

The thicker crust of the Christie Domain is interpreted to have acted as a buttress against which the western Fowler Domain was exhumed. Apparent vertical offset on the eastern boundary fault to the Tallacootra Shear Zone amounts to <5 km. Cumulative apparent vertical movements on reactivated SZ_{2-R4} structures within an 18 km wide zone, from the peak of the positive Bouguer anomaly to the gravity trough within the Christie Domain, amounts to >35 km exhumation corresponding to a westward-decreasing Bouguer gravity gradient of 1.7 μm s^{-2} km^{-1} (Fig. 10). A garnet-biotite gneiss taken from drillcore (TAL4) within the western Fowler Domain

Table 1
Average specific gravity values for major lithologies within the western Gawler Craton after Direen et al. (2005b) and Thomas et al. (2008).

Lithology	Average specific gravity (kg/m^3)	N
Banded iron formation	3730	6
Amphibolite	2900	10
Intermediate metagranitoids (e.g. Tunkillia Suite)	2900	3
Ifould Suite	2840	4
Felsic granulite	2830	8
Pelite/pelitic gneiss	2800	7
Christie gneiss	2760	16
Felsic gneiss	2760	10
Mafic granulite	2750	5

Measured samples are from outcrops and shallow drillholes.

Table 2
Compilation of magnetic susceptibility data for the Christie and Fowler Domains and Ifould Suite plutons after Teasdale (1997) and Thomas et al. (2008) incorporating data collected for this project.

	Lithology	Range (SI)	Average (SI)	*N*
Ifould Suite	Granite	0.00005–0.05683	0.00817	535
	Granodiorite	0.00115–0.05237	0.01301	94
	Amphibolite	0.00004–0.1	0.0245	302
	Gneissic granite	0.0–0.01631	0.00104	371
	Protomylonitic granite	0.0002–0.01223	0.0048	110
	Granite mylonite (TSZ, ISZ)	0.0	0.0	55
Christie Domain	Undifferentiated granite	0.0–0.01	0.00275	8
	Mulgathing complex metasediments	0.00005–0.0003	0.00019	15
	Mafic gneiss, schist and granulite	0.00012–0.021	0.00172	15
	Mylonite	0.00007–0.00015	0.00011	2
Fowler Domain	Mylonite	0.0006–0.013	0.00653	3
	Mafic gneiss – amphibolite	0.0001–0.028	0.00852	9
	Granite and granite gneiss	0.00005–0.004	0.00205	3
	Pelitic gneiss	0.0–0.006	N/A	17

(Fig. 9a) has a peak metamorphic mineral assemblage that grew at 9.3 ± 3.6 kbar and 750 ± 50 °C, indicating lower crustal conditions (Thomas et al., 2008) and confirming this degree of exhumation.

7. Shear zone evolution

7.1. Tectonic context for outcrops at Lake Tallacootra

The shear zone outcrops at Lake Tallacootra occupy a position, on a north–northwest trending segment of what is a curvilinear structure at the regional-scale (Fig. 1). At this location the northwestern Fowler Domain is impinging upon the eastern Christie Domain (Fig. 9b). This is verified by the correlation of D_4 structures at outcrop where southeast-side-up transpressional movements have caused the Fowler Domain to be thrust over the Christie Domain (Fig. 10). Therefore, the observations made at outcrop are only relevant to this segment of the shear zone, particularly since to the northeast and southwest of this segment, the style of shear zone contact and interpreted crust on either side differs (Fig. 2d). It is also expected that these other shear zone segments preserve different structural histories, and this is likely true for the entire Tallacootra Shear Zone given the interpreted variations in dip direction along its strike length.

A simple, progressive deformation history can be invoked for the structures preserved within Lake Tallacootra as they can all be reconciled with a component of NW–SE oriented shortening. The moderately NE-plunging mineral stretching lineation occurs within a prominent mylonitic C fabric that occurs with north–northeast trending sinistral shears (correlating to Riedel shears at the large-scale), a situation that gives evidence for sinistral, west-up transpression, which has been previously interpreted (Direen et al., 2005b). However, although other interpretations report east-side-up kinematics with a mineral lineation consistent with sinistral movements (e.g. Swain et al., 2005a), they also observed dextral transport into the Tallacootra Shear Zone within aeromagnetic data at the regional-scale and considered dextral transpression to typify this structure. Both these previous interpretations present contrasting regional kinematics (based on the most obvious observations at outcrop and regional-scales), which are individually valid, however more thorough analysis at several scales has been required in order to constrain the overall kinematics of polydeformation that has been alluded to, but not addressed for the Tallacootra Shear Zone (Swain et al., 2005a; Direen et al., 2005b; Fraser and Lyons, 2006; Thomas et al., 2008). Incorporation of the detailed outcrop analysis with the regional overprinting and kinematic framework has provided a multistage evolution, which is substantiated by the published evidence, and reconciles the observations at all scales.

7.2. Correlation of shear zone evolution from the outcrop to the regional-scale

Conflicting shear sense indicators prevent accurate kinematic analysis of second generation shear fabrics. However, S_2 is geometrically related to the deformation and lithological distribution of interpreted ca. 1680 Ma Ifould Suite granitic melts, which are strongly flattened parallel to these structures. Regionally, the northwestern margin of the Fowler Domain contains sets of interpreted elongated plutons bound by domain boundary-parallel dip–slip shear zones (SZ_1) providing a large-scale correlative to S_2 C-surfaces at outcrop. S_2 fabrics within the Tallacootra Shear Zone have strikes oblique to the orientation of the shear zone, and appear more closely related to the trend of SZ_1 within the northwestern Fowler Domain (Fig. 9b). If this correlation is correct, D_2 shearing predates movement on the Tallacootra Shear Zone and is likely related to convergence between an interpreted Palaeoproterozoic rift basin within the Fowler Domain and the Christie Domain.

The angular relationships between S_2 and S_3 at outcrop (Figs. 9c,d) and the kinematics of overprinting D_3 shear zones match the overprinting relationships between SZ_1 and SZ_2 as seen in aeromagnetic datasets (Fig. 9c). At outcrop D_3 structures trend north–northeast and perturb the trajectory of D_2 structures (S_2, Lm_2/F_2) with counterclockwise rotations on a vertical axis, consistent with sinistral strike-slip movements within the shear zone. However, the D_3 displacements at outcrop do not indicate large horizontal transports as is suggested by the regional geophysical datasets (Fig. 2d), which image a major negative magnetic anomaly ~400 m east of outcrops within Lake Tallacootra (Fig. 9a) corresponding to ~40 km of sinistral strike-slip. Therefore the shear zone pattern observed at outcrop is interpreted as the manifestation of distributed strain within the footwall block of the Tallacootra Shear Zone consistent with the partitioning of strain into a major boundary fault that coincides with regional aeromagnetic and gravity gradients as well as the boundary between the Christie and Fowler Domains (Fig. 10).

NE–SW extension (subparallel to S_2) is required for the S_3 orientation to be reactivated under dilation during the emplacement of aplite, into S_3-parallel and S_2-orthogonal zones. Accurate geochronology of this lithology will constrain this period of activity when NW–SE oriented shortening switched to NE–SW oriented extension after D_3.

Northwest-dipping SZ_3 shear zones (Fig. 9b) do not have an observed expression within Lake Tallacootra. At the regional-scale these structures appear kinematically linked to steeply dipping reverse faults with southeast-directed transport directions (Fig. 9b). These structures are overprinted by east-side-up movements on the Tallacootra Shear Zone, which coincides with the latest ductile deformation observed within the Lake Tallacootra (D_4) and has been modeled at the lithospheric scale (Fig. 10). Partitioned reactivation of S_2 fabrics caused the refolding of F_2 into non-cylindrical geometries in concert with a steeply northeast-plunging extensional axis as evidenced by late, well developed mineral lineations in the plane of S_2. Clockwise rotation of D_3 aplite dykes and the development of dextral buckle folds indicate a component of regional dextral strike-slip reinforcing the interpretation of a lithospheric positive flower structure within the northwestern Fowler Domain, to which the Tallacootra Shear Zone

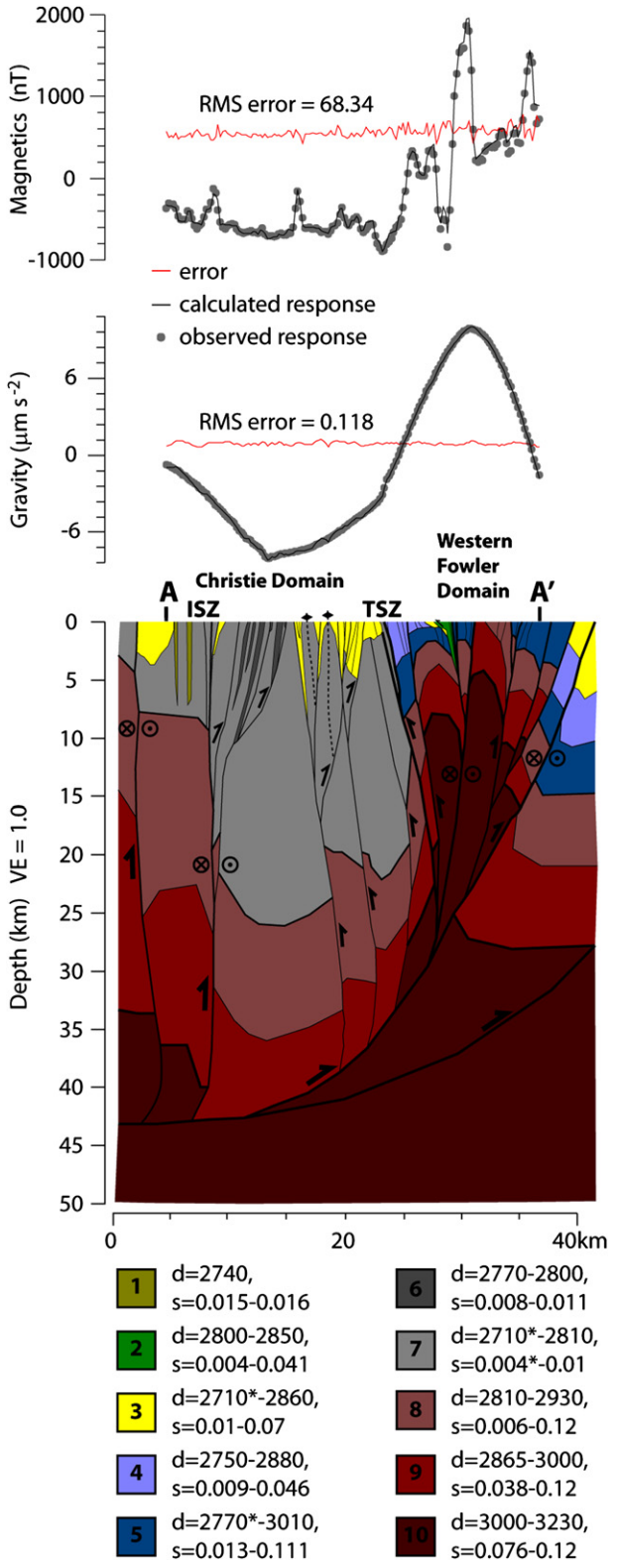

Fig. 10. 2D lithospheric scale forward model of the aeromagnetic and Bouguer gravity data along profile *A*–*A*′. Modeled lithologies are labeled with their range in magnetic susceptibility (SI) and density (kg m^{-3}). * = reduced density coincident with shear zones. Lithologies are: (1) Gairdner Dyke; (2) dense basic intrusion; (3) Ifould Suite plutons; (4) undifferentiated Fowler Domain sediments; (5) dense, highly magnetic, granulite facies metasediments and mafic sills; (6) magnetic Mulgathing Complex; (7) undifferentiated Mulgathing Complex; (8) Archaean middle crust; (9) Archaean lower crust; (10) sub-continental lithospheric mantle.

constitutes the reactivated northwestern boundary fault and the contact zone between the Christie and Fowler Domains.

7.3. Regional-scale vorticity

Vorticity is a measure of the non-coaxiality within high strain zones (e.g. Bobyarchick, 1986; Tikoff and Fossen, 1995; Kurz and Northrup, 2008). The kinematic vorticity number, W_k, has been shown to exhibit a relationship with the angle α between two eigenvectors (Bobyarchick, 1986), one corresponding to the shear zone boundary (Simpson and De Paor, 1993) and the other corresponding to the inclined flow apophysis, which shear bands or C′ fabrics are interpreted to parallel (e.g. Bobyarchick, 1986; Pray et al., 1997). W_k is dependent on the magnitude of α and ranges from zero for pure shear to one for simple shear being simply expressed as:

$$W_k = \cos\alpha \quad (1)$$

The non-conventional methods applied here incorporate the use of data at several scales to infer the boundary conditions of shearing under the assumption that simplified bulk shear is scale invariant (e.g. Turcotte, 1989; Hippertt, 1999). The calculation of W_k is also made with the assumptions that deformation occurred under plane strain conditions, material properties are homogeneous throughout the shear zone, and that the flow apophyses did not rotate during progressive deformation. Thus only a very coarse estimate of vorticity can be assumed and we have only attempted the calculations for D_3 and D_4 shear zone movements which preserve the most coherent fabric relationships as summarized in Fig. 11.

For D_3 shearing on the Tallacootra Shear Zone we have inferred α as the angle between the orientation of D_3 shear zones at outcrop (i.e. C′) and interpreted regional-scale counterparts expressed as SZ_2 shear zone boundaries (i.e. C-plane parallel), which corresponds to an angle of 12° (Fig. 11b). Using Eq. (1), $W_k = 0.97$ for D_3 shearing on the Tallacootra Shear Zone, suggesting near-ideal simple shear behaviour (Bobyarchick, 1986) during subvertical counterclockwise rotations and sinistral strike-slip.

The same analysis was performed at the macroscale on an oriented sample of granitic mylonite recording a very strong NE-plunging D_4 mineral lineation and fabrics interpreted to represent $SZ_{2\text{-}R4}$ shear zone movement. Rotated δ- and σ-porphyroclasts and C′ fabrics indicate southeast-side-up movements. Following the method used above, the angle between *C* and *C*′ is equal to α and is 18° (Fig. 11c). This corresponds to a W_k of 0.95, also within the field of ideal simple shear with a shallowly plunging vorticity vector. These estimates of vorticity demonstrate a very strong component of simple shear operating within the Tallacootra Shear Zone during D_3 and reactivation during D_4.

7.4. Kinematic evolution of the Tallacootra Shear Zone and correlation with the event framework for the western Gawler Craton

We have constrained the kinematics within the Tallacootra Shear Zone for two major regional deformation events (D_3 and D_4). We also demonstrate an episode of extension and coincident magmatism that occurred between these two events. The local deformation phases are correlated to the regional event framework of Hand et al. (2007) and are presented in Table 3.

D_1 and D_2 events predate movement on the Tallacootra Shear Zone. D_1 is constrained to metamorphism within the Christie Domain during the Sleafordian Orogeny (Swain et al., 2005a). D_2 shearing is likely related to convergence between a Palaeoproterozoic sedimentary basin with reduced basement thickness (constituting the Fowler Domain) and the Christie Domain during

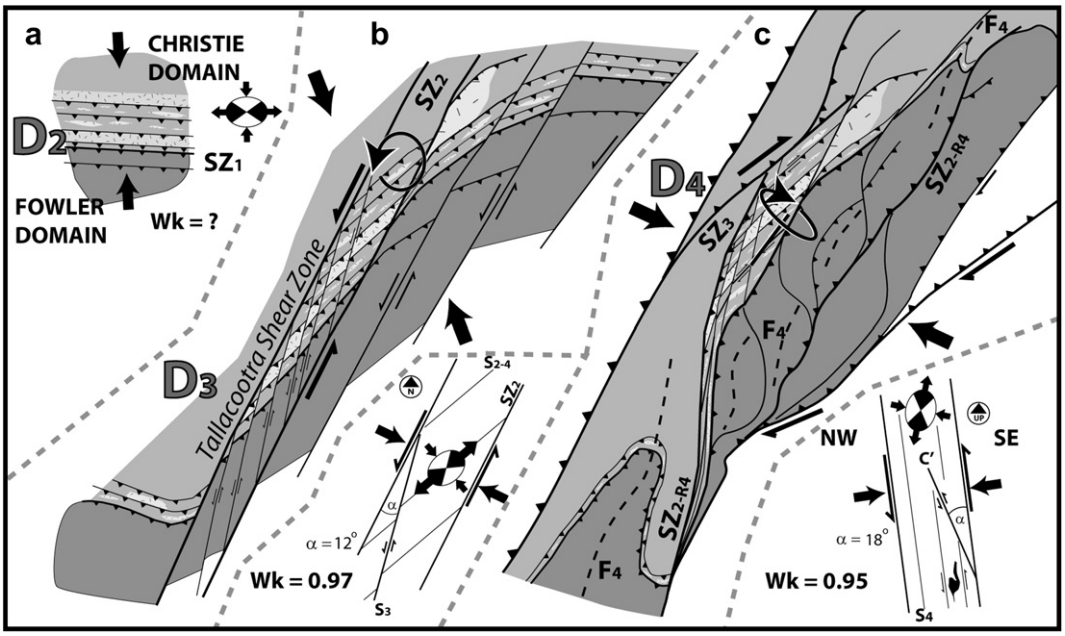

Fig. 11. Schematic evolution of the Tallacootra Shear Zone. (a) D_2 shortening at the margin between the Christie and Fowler Domains. N–S component of shortening based on reconstructing the deformed blocks adjacent to the Tallacootra Shear Zone. (b) Overprinting and counterclockwise rotation of D_2 sheared margin by sinistral strike-slip (D_3) on the Tallacootra Shear Zone. Fabric elements used for calculation of W_k shown in inset. (c) Reactivation of the Tallacootra Shear Zone during D_4 under NW–SE shortening. Regional-scale folds accompanied the exhumation of the northwestern Fowler Domain during dextral transpression. Fabric elements used for calculation of W_k shown in inset.

the latter stages of the Kimban Orogeny. Within the western Gawler Craton we attribute this event to a strong component of N–S oriented pure shear and associated shear zone flattening with minor partitioned simple shear (Fig. 11a). This contrasts with well constrained evidence for dextral transpression within the south-eastern Gawler Craton (Vassallo and Wilson, 2002) indicating variable tectonic boundary conditions within the Kimban Orogen.

Movement on the Tallacootra Shear Zone initiated during D_3 regional deformation (Fig. 11b). A sinistral translation of the Christie–Fowler Domain boundary of ~40 km was accommodated within a broad zone bound by major strike-slip faults. Offsets between boundary faults was minimal and partitioned on oblique D_3 shear zones that aided the asymmetric boudinage of S_2 and support a riedel orientation within the shear zone (Fig. 11b). D_3 became the driver for S_2-parallel (NE–SW) extension required for the emplacement of aplite into the shear zone. This transient episode is corroborated by kinematic evidence for the emplacement of 1595–1575 Ma Hiltaba Suite plutons within the central Gawler Craton under ENE–WSW extension (McLean and Betts, 2003).

S_3 fabrics within Lake Tallacootra outcrops were overprinted during D_4 (Fig. 8). Small components of dextral simple shear were partitioned within reactivated S_2 planes and a coupled steep component of extrusion, verified by steeply plunging lineations and co-parallel F_4 fold axes, indicates constriction under transpressional conditions (Fig. 11c). The dextral strike-slip component and northwest-plunging lineation is consistent with east-side-up kinematic indicators at outcrop. These kinematics are verified by forward modeling, where there is evidence for >35 km vertical offset within the Tallacootra Shear Zone (Fig. 10). The interpretation (Fig. 9b) and modeling indicates that the Tallacootra Shear Zone forms the northwestern boundary of a lithospheric positive flower structure that gives evidence for dextral transpression within the northwestern Fowler Domain. D_4 is the latest ductile event recorded in outcrop at Lake Tallacootra, correlating to the regional cooling between ca. 1470 and 1450 Ma (Fraser and Lyons, 2006) during the Coorabie Orogeny (Hand et al., 2007).

Table 3
Correlation of deformation phases observed at outcrop within the Tallacootra Shear Zone with coincident fabric generations and interpreted regional shear zone overprinting events.

	Fabric generation at outcrop	Regional SZ generation	Kinematics	Event correlation
D_1	S_1	?	?	Sleafordian Orogeny
D_2	S_2	SZ_1	North-directed transport, strong flattening	Kimban Orogeny
D_3	S_3	SZ_2	NW–SE shortening, sinistral strike-slip	?
post-D_3	Aplite dykes	N/A	NW–SE extension	Hiltaba Event
D_4	S_4	SZ_3	Tallacootra SZ = E-up dextral transpression; regionally SE-directed high angle thrusting	Coorabie Orogeny

Kinematics are summarized and correlated with the established event framework of Hand et al. (2007).

8. Conclusions

The multi-scale analysis of mapped and interpreted structural overprinting relationships associated with the Tallacootra Shear Zone has allowed the interpretation of a constrained structural framework and relative overprinting chronology. The use of aeromagnetic and gravity datasets for interpreting subsurface deformation has proven invaluable in this poorly exposed region and supports the following conclusions.

The prominent mylonitic fabric in outcrops within Lake Tallacootra formed under N–S shortening (D_2) prior to the development of the Tallacootra Shear Zone and record interpreted Kimban-aged deformation at the Christie–Fowler Domain boundary (SZ_1). The Tallacootra Shear Zone (SZ_2) initiated during D_3 and sinistrally

offset and deformed the Christie–Fowler Domain boundary and interpreted Ifould Suite plutons by approximately 40 km under partitioned near-ideal simple shear. This deformation was accompanied by counterclockwise rotations of the northwestern Fowler Domain. An extensional episode, previously undocumented in these rocks, led to the emplacement of aplite dykes into the shear zone under NE–SW oriented dilation. This extension correlates regionally to the Hiltaba magmatic event. Reactivation of fabrics within the Tallacootra Shear Zone under renewed NW–SE shortening and dextral transpression saw the development of a positive flower structure and >35 km of exhumation within the northwestern Fowler Domain during the Coorabie Orogeny. Forward modeling shows that transpression occurred in a zone coincident with thinned middle and lower crust adjacent to a thickened Archaean crustal block. The Tallacootra Shear Zone splays off a system of west-dipping shear zones that penetrate the crust and sole into a lithospheric detachment at ~43 km depth.

Acknowledgements

This research was conducted as part of an ARC Linkage funded project (LPO454301) in collaboration with Primary Industries and Resources, South Australia (PIRSA). We would like to thank Neil Chalmers and Anthony Reid at PIRSA and Kate Lloyd at the Department for Environment and Heritage, South Australia. T. Blenkinsop, an anonymous reviewer and H. Williams are thanked for helping to improve the manuscript.

References

Bauer, K., Trumbull, R.B., Vietor, T., 2003. Geophysical images and a crustal model of intrusive structures beneath the Messum ring complex, Namibia. Earth and Planetary Science Letters 6829, 1–16.

Betts, P.G., Giles, D., 2006. The 1800–1100 Ma tectonic evolution of Australia. Precambrian Research 144, 92–125.

Betts, P.G., Valenta, R.K., Finlay, J., 2003. Evolution of the Mount Woods Inlier, northern Gawler Craton, southern Australia; an integrated structural and aeromagnetic analysis. Tectonophysics 366, 83–111.

Bobyarchick, A.R., 1986. The eigenvalues of steady flow in Mohr space. Tectonophysics 122, 35–51.

Butler, R., Tavarnelli, E., Grasso, M., 2006. Structural inheritance in mountain belts: an Alpine–Apennine perspective. Journal of Structural Geology 28, 1–16.

Carreras, J., Druguet, E., Griera, A., 2005. Shear zone-related folds. Journal of Structural Geology 27, 1229–1251.

Culshaw, N., Purves, M., Reynolds, P., Stott, G., 2006. Post-collisional upper crustal faulting and deep crustal flow in the eastern Wabigoon subprovince of the Superior Province, 145. evidence from structural and $^{40}Ar/^{39}Ar$ data from the Humboldt Bay High Strain Zone. Precambrian Research, Ontario. 272–288.

Czeck, D.M., Hudleston, P.J., 2003. Testing models for obliquely plunging lineations in transpression: a natural example and theoretical discussion. Journal of Structural Geology 25, 959–982.

Daly, S., Tonkin, D.G., Purvis, A.C., Shi, Z., 1994. Colona Drilling Program. Mines & Energy, South Australia Open File Envelope, p. 8768.

Daly, S.J., Fanning, C.M., Fairclough, M.C., 1998. Tectonic evolution and exploration potential of the Gawler Craton, South Australia. AGSO Journal of Australian Geology and Geophysics 17, 145–168.

Direen, N.G., Brock, D., Hand, M., 2005a. Geophysical testing of balanced cross sections of fold-thrust belts with potential field data: an example from the Fleurieu Arc of the Delamerian Orogen, South Australia. Journal of Structural Geology 27, 964–984.

Direen, N.G., Cadd, A.G., Lyons, P., Teasdale, J.P., 2005b. Architecture of Proterozoic shear zones in the Christie Domain, western Gawler Craton, Australia: geophysical appraisal of a poorly exposed orogenic terrane. Precambrian Research 142, 28–44.

Elías-Hererra, M., Ortega-Gutiérrez, F., 2002. Caltepec fault zone: an Early Permian dextral transpressional boundary between the Proterozoic Oaxacan and Paleozoic Acatlan complexes, southern Mexico, and regional tectonic implications. Tectonics 21, 1013.

Fanning, C.M., 1997. Geochronological Synthesis of Southern Australia, Part II, The Gawler Craton. South Australia Department of Mines and Energy, Open File Envelope, 8918.

Fanning, C.M., Reid, A.J., Teale, G.S., 2007. A Geochronological Framework for the Gawler Craton, South Australia. South Australia Geological Survey, Bulletin. 55.

Ferris, G.M., Schwarz, M.P., 2004. Definition of the Tunkillia Suite, western Gawler Craton. MESA Journal 34, 32–41.

Ferris, G.M., Schwarz, M.P., Heithersay, P., 2002. The geological framework distribution and controls of Fe-oxide and related alteration, and Cu–Au mineralisation in the Gawler Craton, South Australia. Part I: geological and tectonic framework. In: Porter, T.M. (Ed.), Hydrothermal Iron Oxide Copper-gold and Related Deposits: a Global Perspective 2. Porter GeoConsultancy Publishing, Adelaide, pp. 9–31.

Fraser, G.L., Lyons, P., 2006. Timing of Mesoproterozoic tectonic activity in the northwestern Gawler Craton constrained by $^{40}Ar/^{39}Ar$ geochronology. Precambrian Research 151, 160–184.

Ghosh, S.K., Sengupta, S., 1984. Successive development of plane noncylindrical folds in progressive deformation. Journal of Structural Geology 6, 703–709.

Hand, M., Reid, A., Jagodzinski, E.A., 2007. Tectonic framework and evolution of the Gawler Craton, Southern Australia. Economic Geology 102, 1377–1395.

Hanmer, S., 1997. Shear zone reactivation at granulite facies; the importance of plutons in the localization of viscous flow. Journal of the Geological Society, London 154, 111–116.

Hippertt, J., 1999. Are S–C structures, duplexes and conjugate shear zones different manifestations of the same scale-invariant phenomenon? Journal of Structural Geology 21, 975–984.

Holdsworth, R.E., Butler, C.A., Roberts, A.M., 1997. The recognition of reactivation during continental deformation. Journal of the Geological Society, London 154, 73–78.

Holdsworth, R.E., Hand, M., Miller, J.A., Buick, I.S., 2001. Continental reactivation and reworking: an introduction. In: Holdsworth, R.E., Hand, M., Miller, J.A., Buick, I.S. (Eds.), Continental Reactivation and Reworking. Geological Society London, Special Publications. The Geological Society of London, London, pp. 1–12.

Jessell, M.W., Valenta, R.K., 1996. Structural geophysics: integrated structural and geophysical mapping. In: DePaor, D.G. (Ed.), Structural Geology and Personal Computers. Elsevier Science Ltd, Oxford, pp. 303–324.

Jessell, M., Valenta, R.K., Jung, G., Cull, J.P., Geiro, A., 1993. Structural geophysics. Exploration Geophysics 24, 599–602.

Jones, R.R., Tanner, P.W., 1995. Strain partitioning in transpression zones. Journal of Structural Geology 17, 793–802.

Kurz, G.A., Northrup, C.J., 2008. Structural analysis of mylonitic rocks in the Cougar Creek Complex, Oregon–Idaho using the porphyroclast hyperbolic distribution method, and potential use of SC′-type extensional shear bands as quantitative vorticity indicators. Journal of Structural Geology 30, 1005–1012.

Lin, S., Jiang, D., 2001. Using along-strike variations in strain and kinematics to define the movement direction of curved transpressional shear zones: an example from northwestern Superior Province, Manitoba. Geology 29, 767–770.

Mandal, N., Samanta, S.K., Chakraborty, C., 2004. Problem of folding in ductile shear zones: a theoretical and experimental investigation. Journal of Structural Geology 26, 475–489.

McLean, M.A., Betts, P.G., 2003. Geophysical constraints of shear zones and geometry of the Hiltaba Suite granites in the western Gawler Craton, Australia. Australian Journal of Earth Sciences 50, 525–541.

Myers, J.S., Shaw, R.D., Tyler, I.M., 1996. Tectonic evolution of Proterozoic Australia. Tectonics 15, 1431–1446.

Nabighian, M.N., Grauch, V.J., Hansen, R.O., LaFehr, T.R., Li, Y., Peirce, J.W., Phillips, J.D., Ruder, M.E., 2005. The historical development of the magnetic method in exploration. Geophysics 70, 33–61.

Parker, A.J., Hughes, F.E., 1990. Precambrian provinces of South Australia; tectonic setting Geology of the mineral deposits of Australia and Papua New Guinea; Vol. 2. Monograph Series – Australasian Institute of Mining and Metallurgy 14, 985–990.

Parker, A.J., Lemon, N.M., 1982. Reconstruction of the early Proterozoic stratigraphy of the Gawler Craton, South Australia. Journal of the Geological Society of Australia 29, 221–238.

Parker, A.J., Preiss, W.V., Rankin, L.R., 1993. The Precambrian. In: Drexel, J.F., Preiss, W.V., Parker, A.J. (Eds.), The Geology of South Australia. Bulletin – Geological Survey of South Australia, pp. 8–31.

Payne, J.L., 2008. Palaeo- to Mesoproterozoic evolution of the Gawler Craton, Australia: geochronological, geochemical and isotopic constraints. Ph.D. thesis, Adelaide University.

Pray, J.R., Secor, D.T., Sacks, P.E., Maher, H.D., 1997. Rotation of fabric elements in convergent shear zones, with examples from the southern Appalachians. Journal of Structural Geology 19, 1023–1036.

Simpson, C., De Paor, D.G., 1993. Strain and kinematic analysis in general shear zones. Journal of Structural Geology 15, 1–20.

Swain, G., Hand, M., Teasdale, J., Rutherford, L., Clark, C., 2005a. Age constraints on terrane-scale shear zones in the Gawler Craton, southern Australia. Precambrian Research 139, 164–180.

Swain, G., Woodhouse, A., Hand, M., Barovich, K.M., Schwarz, M.P., Fanning, C.M., 2005b. Provenance and tectonic development of the late Archaean Gawler Craton; U–Pb zircon, geochemical and Sm–Nd isotopic implications. Precambrian Research 141, 106–136.

Teasdale, J.P., 1997. Methods for understanding poorly exposed terranes: the interpretive geology and tectonothermal evolution of the Western Gawler Craton. Ph.D. thesis. Adelaide University.

Thomas, J.L., Direen, N.G., Hand, M., 2008. Blind orogen: integrated appraisal of multiple episodes of Mesoproterozoic deformation and reworking in the Fowler Domain, western Gawler Craton, Australia. Precambrian Research 166, 263–282.

Tikoff, B., Fossen, H., 1995. The limitations of three-dimensional kinematic vorticity analysis. Journal of Structural Geology 17, 1771–1784.

Tomkins, A.G., Dunlap, W.J., Mavrogenes, J.A., 2004. Geochronological constraints on the polymetamorphic evolution of the granulite-hosted Challenger gold

deposit: implications for assembly of the northwest Gawler Craton. Australian Journal of Earth Sciences 51, 1–14.
Turcotte, D.L., 1989. Fractals in geology and geophysics. Pure and Applied Geophysics 131, 171–176.
Vassallo, J.J., Wilson, C.J.L., 2001. Structural repetition of the Hutchison Group metasediments, Eyre Peninsula, South Australia. Australian Journal of Earth Sciences 48, 331–345.
Vassallo, J.J., Wilson, C.J.L., 2002. Palaeoproterozoic regional-scale non-coaxial deformation; an example from eastern Eyre Peninsula, South Australia. Journal of Structural Geology 24, 1–24.
Watterson, J., 1975. Mechanism for the persistence of tectonic lineaments. Nature 253, 520–522.
Webb, A.W., Thomson, B.P., Blisset, A.H., Daly, S.J., Flint, R.B., Parker, A.J., 1986. Geochronology of the Gawler Craton, South Australia. Australian Journal of Earth Sciences 33, 119–143.
Whiting, T.H., 1986. Aeromagnetics as an aid to geological mapping-a case history from the Arunta Inlier, Northern Territory. Australian Journal of Earth Sciences 33, 271–286.
Williams, H.A., Betts, P.G., 2009. The Benagerie Shear Zone: 1100 Ma of reactivation history and control over continental lithospheric deformation. Gondwana Research 15, 1–13.
Woodcock, N.H., Rickards, B., 2003. Transpressive duplex and flower structure: Dent Fault System, NW England. Journal of Structural Geology 25, 1981–1992.